Smooth Profile Generation for a Tile Printing Machine

Corrado Guarino Lo Bianco and Roberto Zanasi, *Associate Member, IEEE*

***Abstract*—In this paper a digital filter is proposed for the generation of smooth set points for motion control systems. The proposed nonlinear filter produces profiles with bounded velocity and acceleration starting from rough reference signals (steps and ramps). An actual implementation of the filter for a tile printing machine is presented and experimental results are reported.**

***Index Terms*—Discrete-time filters, motion planning, nonlinear filters, smoothing methods, time-optimal control, tracking filters.**

I. Introduction

SYNTHESIS of smooth profiles is an important issue in motion control applications, especially when high-level performance is required. This is the case with many industrial applications where fast dynamics and high precisions are required for systems with large inertias and frictions. When rough set points (i.e., steps or ramps) are used, large torques are required to obtain fast dynamics from these systems: this is unsatisfactory from an engineering viewpoint. A proper alternative is the use of smooth set-point profiles (i.e., velocity and acceleration bounded), aiming to limit the torque amplitude while guaranteeing good performances.

This problem is well known in robotics where motion profiles are normally evaluated offline, ensuring continuity in the velocity and, when possible, also in the acceleration profiles [1]. If an optimization procedure is available, trajectories can also be computed to obtain minimum time performances [2] and torque boundness [3]. For the same reason, in motion control systems spline, linear-quadratic profiles, etc., are commonly used for generating smooth electrical axes. A recent approach to this problem is based on the principle of system inversion [4] [5]: given the plant model, the reference signal is evaluated to obtain fast dynamics, with bounded (or null) overshoot, also taking into account the actuators limits [6].

In all the above approaches the smooth profiles are evaluated offline and only step reference signals are considered. With the smooth profile generator proposed in this paper both these limits are dropped. Smooth profiles are evaluated online by means of a dynamic system, so that they can also be changed while controlling the actual system. For this reason the profile generator is particularly indicated for applications where the rough reference signal is not known *a priori*.

The basic scheme of this generator has been described in [7]–[9] where both the continuous-time and the discrete-time implementations are reported. It is based on a nonlinear state variable filter that computes minimum-time smooth profiles starting from rough signals (ramps and steps are considered in this paper). The rough reference signal is always reached without overshoot and with zero tracking error. The smooth output of the filter has the first and the second derivatives (velocity and acceleration) bounded with bounds that can be freely changed, even online. Moreover, the first and second time derivatives of the smooth reference signal are always available as outputs of the filter and can be usefully used for adding feedforward actions in the control system.

In this paper an improved version of the digital filter is presented, particularly suitable for applications where bounds on the velocity and on the acceleration need to be continuously changed. Moreover, an actual implementation of the filter for a tile printing machine is presented. In Section II, the specifications for the filter design are obtained by considering the actual control problem (CP). Section III reports the filter structure. In Section IV, the experimental results obtained from the actual plant are reported and discussed, while conclusions are drawn in Section V.

II. Control Problem

The tile printing machine described in the following represents a typical application where the proposed smoothing filter can be used to improve the control performances. The profile generator is suited for applications where rough set-point signals need to be smoothed in order to bound transient dynamics. A typical case is the generation of electrical axes for servomechanisms where piecewise-continuous reference signals (such as ramps or constants) need to be properly joined.

The tile printing machine is mainly constituted by an inked roller whose surface bears one or more images to be impressed on some tiles carried by a conveyer belt. For example, in Fig. 1 three images (indicated by the dark sectors) are impressed on the printing roller. The distance between two adjacent images (in the following described as "nonprinting sector") will be indicated with d_1, while the distance between two adjacent tiles will be indicated by d_2. Tiles are randomly supplied to the conveyer belt, so that d_2 is variable and, in general, is different from d_1. Tiles arrival is detected by means of a laser sensor. Each time a tile is detected, an electrical axis (a ramp) is generated for the roller in order to obtain a perfect alignment between images

Manuscript received November 14, 2001; revised June 24, 2002. Abstract published on the Internet March 4, 2003.

C. Guarino Lo Bianco is with the Dipartimento di Ingegneria dell'Informazione, University of Parma, 43100 Parma, Italy (e-mail: guarino@ce.unipr.it).

R. Zanasi is with the Dipartimento di Ingegneria dell'Informazione, University of Modena and Reggio Emilia, 41100 Modena, Italy (e-mail: roberto.zanasi@unimo.it).

Digital Object Identifier 10.1109/TIE.2003.812284

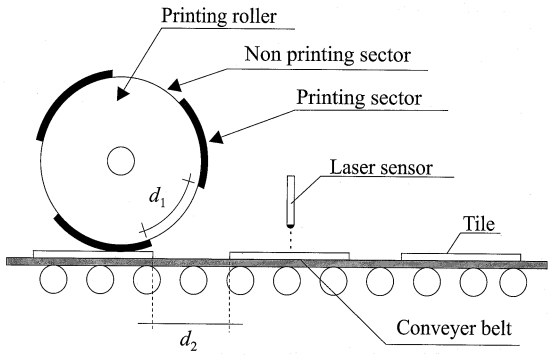

Fig. 1. Scheme of the tile printing machine.

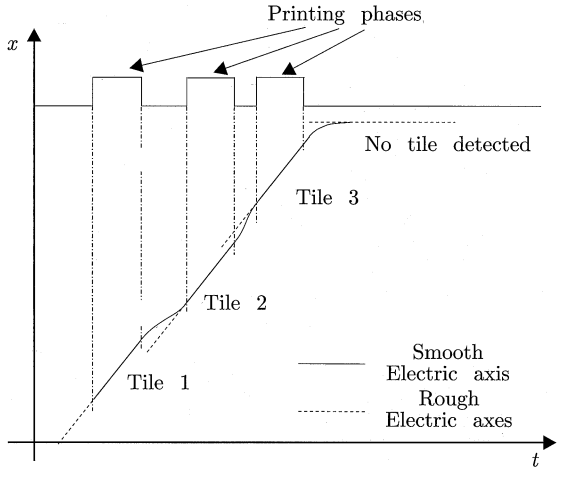

Fig. 2. Typical electrical axes for the printing roller. Note the different alignment between various axes owing to the random distribution of the tiles.

and tiles (a precision of $\pm 0.1 \times 10^{-3}$ m is required). The slope of the electrical axis depends on the conveyer belt speed. If no tile is detected, the roller must be stopped in order to wait for new arrivals. Fig. 2 shows all possible situations. Let us indicate the roller reference signal by x (angular position). Dashed lines represent the rough set points while the squared signal indicates the phases along with tiles are printed. During these phases a perfect alignment between printing roller and tiles needs to be guaranteed, while transients between adjacent electrical axes are allowed exclusively during nonprinting phases. In the example of Fig. 2, the distance between tiles 1 and 2 is greater than d_1 (i.e., $d_2 > d_1$), so that the printing roller needs to be braked in order to get the alignment with the second axis. The opposite situation occurs during the next transient $(d_2 < d_1)$. After the third tile is printed, the roller is stopped until the laser sensor detects new arrivals.

Normally, d_2 is chosen as small as possible to increase the productivity. As a result, transients between electrical axes have to be very fast and precise in order to guarantee a perfect alignment at the beginning of each printing phase. This target can be reached only by smoothly joining all the reference signals.

Keeping in mind our application, it is possible to propose proper requirements for the smooth profile generator. First of all, smooth profiles need to be updated at each transient because d_2 changes randomly. Secondly, transient dynamics (i.e. acceleration and velocity of the reference signal) need to be bounded to

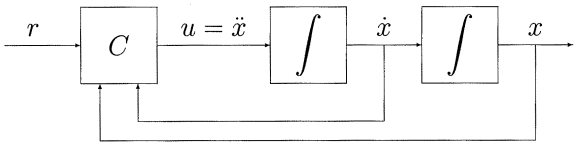

Fig. 3. Basic scheme of the nonlinear trajectory smoother: r reference signal; x output smooth signal; $\dot{x}$ velocity; $\ddot{x}$ acceleration; and u controller output.

reduce the mechanical stress. Such bounds have to be continuously changed to account for the changing operating conditions. To reduce the mechanical stress and to minimize the energy consumption and the size of the roller motor, the entire time interval between two adjacent printing phases must be used to align the roller. In such a way, profiles with smaller acceleration and velocity bounds can be adopted. As a result, each transient requires different bounds for the first $(\dot{x})$ and the second $(\ddot{x})$ time derivatives of the reference signal because transient length depends on the random arrival of the tiles.

It has been previously noted that, at the beginning of each printing phase, the roller has to be perfectly aligned with the current electric axis. This implies that the smooth signal has to join the rough reference with zero error before each printing phase starts. Moreover, the profile generator has to provide the first and the second time derivatives of the smooth set point to improve the position controller performance. Both signals can be usefully used to reduce the transient tracking error thus guaranteeing a precise alignment at the beginning of the printing phase.

The basic scheme of the proposed profile generator is the second-order state variables filter shown in Fig. 3 for the continuous-time implementation. Let us denote with r the rough reference signal and with x the smooth output of the filter. Signals $\dot{x}$ and $\ddot{x}$ correspond, according to Fig. 3, to the first and second time derivatives of the smooth signal x.

Owing to mechanical constraints, the roller velocity always has to be non-negative. Consequently, the absolute value of the velocity lower bound differs from the upper. In particular, the upper bound is selected according to the desired dynamics, while the lower bound is set equal to zero. In the following, the upper and lower velocity bounds will be indicated with $\dot{x}_M^+ \in [0, +\infty)$ and $\dot{x}_M^- \in (-\infty, 0]$, respectively. Moreover, the absolute values of the upper and lower acceleration bounds will be chosen coincident and denoted with $U \in [0, +\infty)$. This restriction is not relevant for the control problem considered and could be easily dropped with a minor change in the filter control law.

All requirements listed above can be converted into constraints for the design of the smooth trajectory generator.

Control Problem:

Design a nonlinear state-variables filter whose output $x(t)$ tracks "at best" the reference signal $r(t)$ with the following specifications.

1) *The first and second time derivatives of the output $x(t)$ must be bounded*

$$\dot{x}_M^- \le \dot{x}(t) \le \dot{x}_M^+, \qquad |\ddot{x}(t)| \le U \tag{1}$$

and the bounds can be time varying and can also change during the transients.

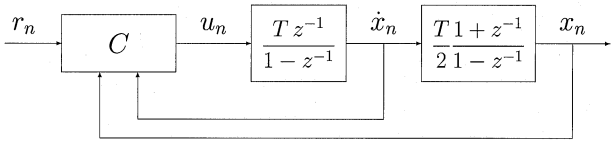

Fig. 4. Discrete-time trajectory smoother.

2) *When a reference signal satisfying relation (1) is applied, the tracking condition $x(t) = r(t)$ is reached in finite time.*
3) *When a discontinuous reference signal is applied (or the reference signal has time derivatives larger than the bound values), the tracking is lost. As soon as the reference signal again satisfies relation (1), the tracking is again achieved in "minimum time" and without overshoot.*
4) *The time derivatives $\dot{x}(t)$ and $\ddot{x}(t)$ of the bounded output must be available for the generation of feedforward actions.*
5) *If the output derivatives $\dot{x}(t)$ and $\ddot{x}(t)$ do not satisfy relation (1), they must be forced again within the bounds in minimum time.*

In the following, the first derivative of the reference signal $\dot{r}$ is assumed to be known. Although this condition ensures some properties when tracking high-order reference signals (ramps, parabolas, etc.) it is not strictly required to track steps or square-wave signals.

The trajectory smoother presented in this work comes directly from that proposed in [9]. A discrete-time implementation is considered because a digital controller is used in the real application.

III. Nonlinear Filter

The block scheme of the discrete-time trajectory smoother is shown in Fig. 4. Two different discrete-time integrators have been used. Variables have the same meanings as in Section II. Subscript "n" indicates sampled variables. The sampling period will be denoted by T.

A version of the trajectory smoother satisfying the first four requirements of the CP, but with symmetric bounds on the velocity ($\dot{x}_M^+ = -\dot{x}_M^- := \dot{x}_M$), is reported and extensively described in [9]. The proposed control law is the following:

$$C1: u_n := -U\text{sat}(\sigma_n)\frac{1+\text{sgn}(\dot{x}_n\text{sgn}\sigma_n + \dot{x}_M - TU)}{2} \quad (2)$$

$$\sigma_n := \dot{z}_n + \frac{z_n}{m} + \frac{(m-1)}{2}\text{sgn}(z_n) \quad (3)$$

$$m := \text{Int}\left[\frac{1+\sqrt{1+8|z_n|}}{2}\right] \quad (4)$$

$$z_n := \frac{1}{TU}\left(\frac{y_n}{T} + \frac{\dot{y}_n}{2}\right) \quad (5)$$

$$\dot{z}_n := \frac{\dot{y}_n}{TU} \quad (6)$$

where $y_n = x_n - r_n$ is the tracking error, $\dot{y}_n = \dot{x}_n - \dot{r}_n$ is the velocity error, $\dot{r}_n$ is the discrete-time derivative of signal r_n, sat$(\cdot)$ is the saturation function, and $\sigma_n = 0$ is the sliding surface. Signals r_n and $\dot{r}_n$ are assumed to be known. Moreover, $\dot{r}_n$ is supposed to be piecewise constant.

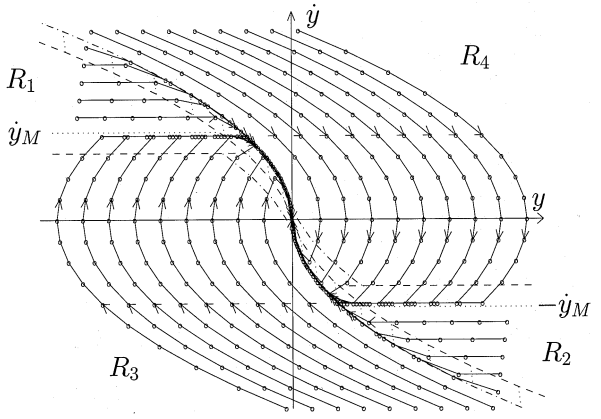

Fig. 5. Phase-plane trajectories for controller C1: circles indicate points corresponding to sampling instants while the dotted-dashed lines evidence the boundary layer.

The behavior of the trajectory smoother can be understood with the help of the phase-plane trajectories (y, $\dot{y}$) shown in Fig. 5. From this figure it is evident that the system state moves always toward the origin (i.e., $x_n \to r_n$ and $\dot{x}_n \to \dot{r}_n$). The proof of the global convergence can be found in [9]. The constraint on the maximum acceleration is satisfied due to the control law (2): $|u_n|$ cannot be larger than U. The bounds on the velocity $\dot{x}$ are satisfied in a finite time owing to the shape of the state trajectories. To understand the system behavior, the phase-plane has been divided into four regions. The trajectories within region $R_3 = \{(y_n, \dot{y}_n) : 0 < u_n \le U\}$ are curves (almost always parabolas) with positive acceleration. In minimum time they reach the maximum velocity $\dot{y}_M$ or the sliding surface $\sigma_n = 0$. Similar considerations hold for region $R_4 = -R_3$. The trajectories within regions $R_1 = \{(y_n, \dot{y}_n) : u_n = 0,\ \dot{y}_n > \dot{y}_M - TU\}$ and $R_2 = -R_1$ reach the sliding surface $\sigma_n = 0$ in finite time, but they do not satisfy in minimum time the constraint on the maximum velocity. This behavior is satisfactory in most cases, but it does not agree with statement 5) of the CP which requires the system to be forced toward the feasible region $|\dot{x}_n| \le \dot{x}_M$ "in minimum time." To cope with this statement, and to deal with the more general case of asymmetric velocity bounds ($\dot{x}_M^+ \neq \dot{x}_M^-$), the following controller $C2$ can be used:

$$u_n := -U\text{sat}(\sigma_n) \quad (7)$$

$$\sigma_n := \begin{cases} \dot{z}_n - \dot{z}_M^+, & \text{if } z_n < z_M^+ \\ \dot{z}_n + \frac{z_n}{m} + \frac{(m-1)}{2}\text{sgn}(z_n), & \text{if } z_M^+ \le z_n \le z_M^- \\ \dot{z}_n - \dot{z}_M^-, & \text{if } z_n > z_M^- \end{cases} \quad (8)$$

where

$$z_M^+ = -\lceil \dot{z}_M^+ \rceil \left[\dot{z}_M^+ - \frac{\lceil \dot{z}_M^+ \rceil - 1}{2}\right] \quad (9)$$

$$\dot{z}_M^+ = \frac{\dot{x}_M^+ - \dot{r}_n}{TU} \quad (10)$$

$$z_M^- = \lceil -\dot{z}_M^- \rceil \left[-\dot{z}_M^- - \frac{\lceil -\dot{z}_M^- \rceil - 1}{2}\right] \quad (11)$$

$$\dot{z}_M^- = \frac{\dot{x}_M^- - \dot{r}_n}{TU} \quad (12)$$

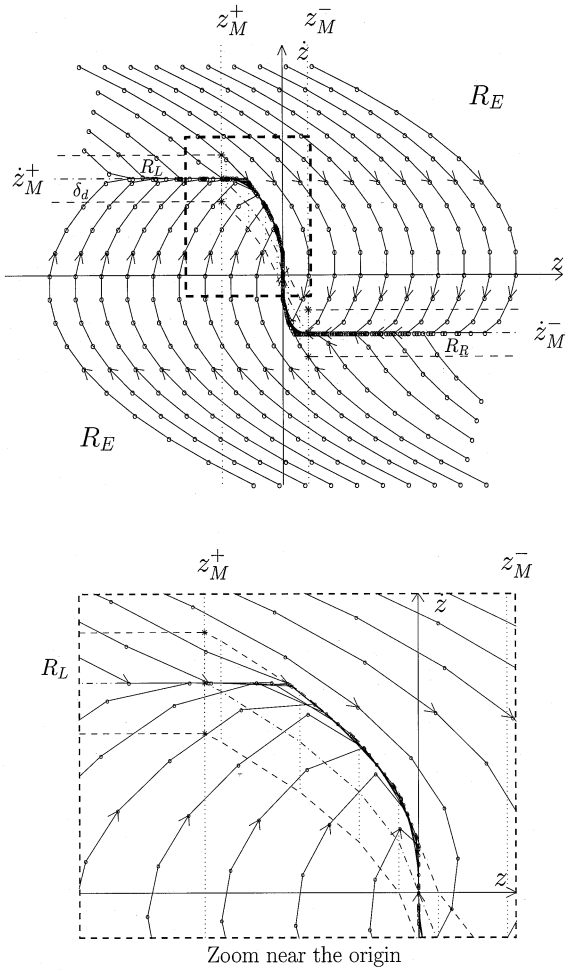

Fig. 6. Phase-plane trajectories for controller $C2$: trajectories in large and zoom in the vicinity of the origin.

where m, z_n, and $\dot{z}_n$ are defined in (4)–(6), and where function $\lceil\cdot\rceil$ provides the upper integer part of its argument. Note that $z_M^+ < 0$ and $z_M^- > 0$. Moreover, note that, according to (5) and (6), the two velocities $\dot{z}_M^+$ and $\dot{z}_M^-$ are the transformed values of the two maximum velocities $\dot{x}_M^+$ and $\dot{x}_M^-$. The phase-plane trajectories, obtained when controller $C2$ is used, are shown in Fig. 6.

Let $\mathbf{z}_n[z_n, \dot{z}_n]^T$ denote the generic point of the phase plane $(z_n\ \dot{z}_n)$. The sliding surface $\delta_d = \{\mathbf{z}_n : \sigma_n = 0\}$ is the curve in the phase plane where the control signal u_n is zero: $u_n = -U\text{sat}(\sigma_n) = 0$. Moreover, the boundary layer $\epsilon_d = \{\mathbf{z}_n : |\sigma_n| < 1\}$ is the region of the phase-plane where the control signal u_n is not saturated: $|u_n| = |-U\text{sat}(\sigma_n)| = |-U\sigma_n| < U$. In Fig. 6, the boundary layer ϵ_d is delimited by the two dashed curves, and the sliding surface δ_d is the dashed-dotted line placed in the center of ϵ_d. The following property holds.

Property 1. Controller $C2$ Solves the Control Problem.

Proof: Let us divide the phase plane into four regions.

I) The region outside the boundary layer: $R_E = \{\mathbf{z}_n : |\sigma_n| \geq 1\}$. The state trajectories starting from R_E are parabolas characterized by the maximum value of the control input, $u_n = \pm U$, and due to the particular shape of the phase-plane trajectories (see Fig. 6) they reach the boundary layer ϵ_d in "minimum time."

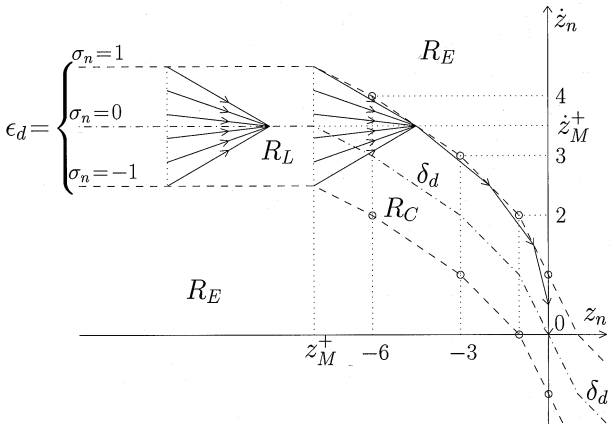

Fig. 7. Phase-plane trajectories within the boundary layer when controller $C2$ is used.

II) The central region of the boundary layer: $R_C = \{\mathbf{z}_n : |\sigma_n| < 1,\ z_M^+ \leq z \leq z_M^-\}$. By comparing (3) with (8), it is possible to conclude that inside region R_C both controllers have the same behavior. Hence, as demonstrated in [9], when the initial state belongs to region R_C the corresponding trajectory reaches the origin in minimum time and without overshoot (see Fig. 7).

III) The left region within the boundary layer: $R_L = \{\mathbf{z}_n : |\sigma_n| < 1,\ z < z_M^+\}$. The dynamic model of the trajectory generator in the $(z, \dot{z})$ phase plane is the following (see [9]):

$$\begin{bmatrix} z_{n+1} \\ \dot{z}_{n+1} \end{bmatrix} = \begin{bmatrix} 1 & 1 \\ 0 & 1 \end{bmatrix} \begin{bmatrix} z_n \\ \dot{z}_n \end{bmatrix} + \begin{bmatrix} \frac{1}{U} \\ \frac{1}{U} \end{bmatrix} u_n. \tag{13}$$

When $\mathbf{z}_n \in R_L$, the control law (7) and (8) provides

$$u_n = -U\left(\dot{z}_n - \dot{z}_M^+\right). \tag{14}$$

Substituting (14) in (13), one obtains

$$\begin{bmatrix} z_{n+1} \\ \dot{z}_{n+1} \end{bmatrix} = \begin{bmatrix} 1 & 0 \\ 0 & 0 \end{bmatrix} \begin{bmatrix} z_n \\ \dot{z}_n \end{bmatrix} + \begin{bmatrix} 1 \\ 1 \end{bmatrix} \dot{z}_m^+. \tag{15}$$

The solution of system (15) when starting from initial condition $\mathbf{z}_n \in R_L$ is the following:

$$\begin{bmatrix} z_{n+d} \\ \dot{z}_{n+d} \end{bmatrix} = \begin{bmatrix} z_n + d\dot{z}_M^+ \\ \dot{z}_M^+ \end{bmatrix}, \qquad d \geq 1 \tag{16}$$

that is, according to (16), the velocity $\dot{z}$ reaches the maximum value $\dot{z}_M^+$ in a single sampling period (i.e., $\dot{z}_{n+1} = \dot{z}_M^+$) and then is kept constant until the state $\mathbf{z}_{n+d}$ reaches (in minimum time) the region R_C. The phase-plane trajectories within the boundary layer are shown in detail in Fig. 7. The point $(z_M^+, \dot{z}_M^+)$ defined in (9) and (10) has been obtained as the intersection of the horizontal line $\dot{z} = \dot{z}_M^+$ with the segmented curve $\dot{z} + (z/m) + [(m-1)/2]\text{sgn}(z) = 0$ [see (8)].

IV) The right region within the boundary layer: $R_R = \{\mathbf{z}_n : |\sigma_n| < 1,\ z > z_M^-\}$. The system behavior within this region is quite similar to the previous case and can be treated in the same way.

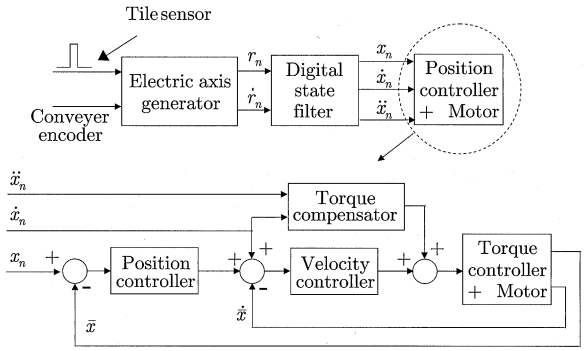

Fig. 8. Motion control scheme.

The previous considerations allow us to conclude that, starting from any state inside regions R_E, R_L, and R_R, the region R_C is reached in minimum time and satisfying the velocity and acceleration constraints. Then, from region R_C, the origin is reached in minimum time and without overshoot (see [9]). The Property is proved. ◇

IV. Experimental Results

The nonlinear state filter has been used to obtain high performance from a commercial controller for tile printing. Discontinuities on electrical axes made it almost impossible to achieve the required precision during the printing phase ($\pm 0.1 \times 10^{-3}$ m) by using standard controllers. Moreover, discontinuities were also the reason for large amplitude peaks in the torque set point given by the position controller.

The overall control scheme and a detail of the inner position controller are shown in Fig. 8. The first block of the overall control scheme generates the nonsmooth electrical axis r_n synchronous with the arriving tile. More precisely, an encoder linked to the conveyer belt and a laser sensor are used to evaluate the tile position and to generate the required axis. The axis slope $\dot{r}_n$ depends on the velocity of the conveyer belt. The signal $\dot{r}_n$ is evaluated by differentiating numerically and low-pass filtering the tile position signal r_n. This simple solution gives optimal results because the conveyor velocity is kept almost constant by means of a velocity controller. The nonsmooth axis is then filtered by the smooth profile generator and the resulting signals are sent to the roller position controller. As shown by the detail of Fig. 8, the roller position is governed by means of a nested position-velocity control loop. Its output is a torque set-point signal used to drive a commercial, torque controlled, brushless motor. The first and second time derivatives of the smooth set point are used to generate feedforward signals for the controller. More precisely, the signals $\dot{x}_n$ and $\ddot{x}_n$ are used to generate an estimate of the torque set-point signal in order to compensate for the roller friction and inertia.

All measurements reported in the following are directly obtained from the analog outputs of the real commercial controller named CND41-Rotoprint and produced by ARTECO s.p.a. (see Fig. 9). The small amplitude noise is due to the error added by the analog acquisition of the signals. The generation of the smooth electrical axis is shown in Fig. 10. The squared signal indicates the time interval along which a tile is being printed.

Fig. 9. CND41-Rotoprint controller.

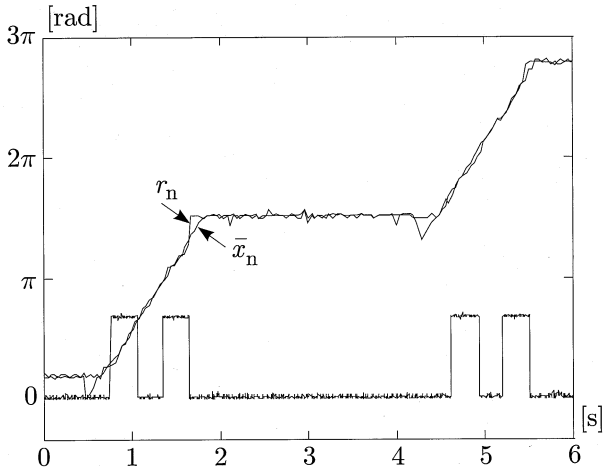

Fig. 10. Nonsmooth axis r_n and the actual roller position $\bar{x}_n$. The squared signal indicates the printing phase of a tile.

During this phase a perfect alignment between the roller and the conveyer axes must be guaranteed. The other two signals represent, respectively, the nonsmooth axis r_n generated by the first block of Fig. 8 and the actual roller position $\bar{x}_n$. In the example shown in Fig. 10, tiles are not equally spaced. Two typical situations are reported. In the first case, tiles arrive almost exactly spaced ($d_1 \cong d_2$) so that only a minor correction is required (the situation is the same reported in Fig. 2 for the transient between tiles 2 and 3). In the second case, the space between tiles is so large that the roller must be stopped. Especially in this case, the action of the nonlinear filter can be appreciated. Indeed, when a new tile is detected the electrical axis becomes strongly discontinuous. Such discontinuities are completely cancelled by the filter.

Fig. 11 shows in detail the first two transients of Fig. 10. As usual, the squared signal indicates the printing phases. Initially, the roller is waiting in one of its parking positions. When a new tile is detected, the state filter generates a smooth profile satisfying the acceleration and velocity bounds. In particular, the sat-

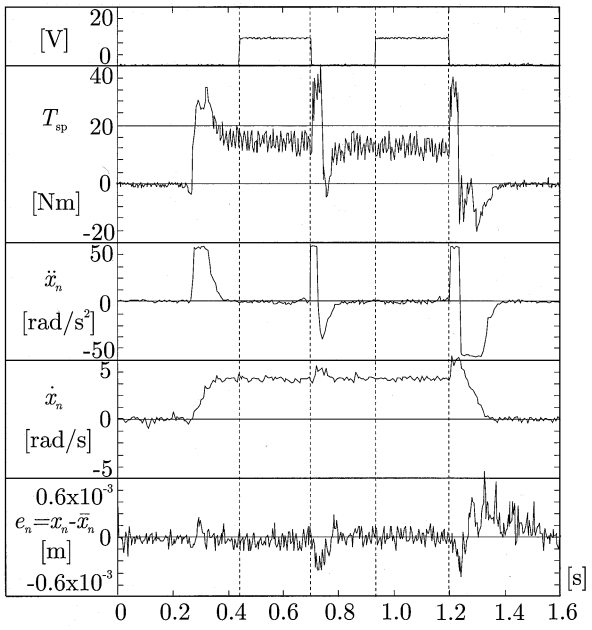

Fig. 11. Detail of some characteristic signals under actual operating conditions. From top to bottom: tile printing signal; torque set point for the motor actuator $T_{\rm sp}$; acceleration signal $\ddot{x}_n$; velocity signal $\dot{x}_n$; and reference tracking error $e_n = x_n - \bar{x}_n$. All signals are measured at the nominal speed of the conveyer belt.

uration on the acceleration signal $\ddot{x}_n$ is evident. When the roller and the tile electrical axes coincide, the acceleration goes to zero and the velocity is constant (see the $\dot{x}_n$ plot). During this phase the tile is being printed. At the end of the printing phase a new tile is sensed: the roller must be aligned with the new axis. After the second tile has been printed, the roller is stopped. The presence of the smooth profile generator strongly improves the performances of the roller position controller. This is evident from the tracking error signal e_n (the difference between the smooth set point x_n and the actual roller position $\bar{x}_n$): error is small not only during tile printing but also during transients. Also, the torque set-point signal $T_{\rm sp}$ shows good characteristics: the required torque during transients is strongly reduced because the acceleration is bounded by the proposed filter. Indeed, the maximum value of $T_{\rm sp}$ is only the double of the torque required to keep constant the velocity during a printing phase.

The velocity and the acceleration signals $\ddot{x}_n$ and $\dot{x}_n$ are shown in Fig. 12 at the maximum conveyer belt velocity. In this case the tile speed is higher, so that higher dynamics are required to achieve the correct alignment on time: bounds on velocity and acceleration are dynamically scaled acting directly on the parameters U and $\dot{x}_M^+$. In general, both U and $\dot{x}_M^+$ are continuously changed depending on the velocity of the conveyer belt and on the distance d_2. The purpose, as stated in Section II, is to obtain a correct alignment with moderate velocities and accelerations. The parameter d_2 is, from this point of view, very critical. If tiles arrive too frequently (i.e., d_2 is too small), the required accelerations could be excessive. This critical situation is revealed by the torque compensator (see Fig. 8) which demands a torque larger than the maximum motor torque, so that the correct alignment cannot be obtained on time.

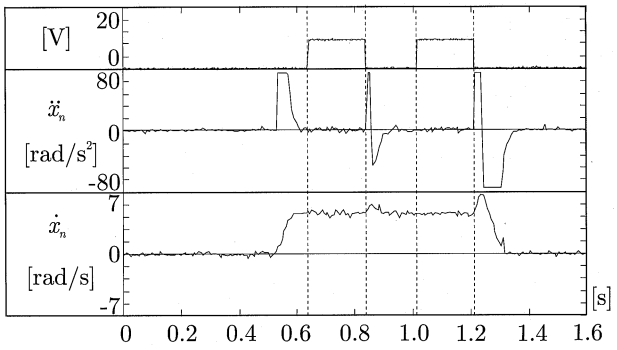

Fig. 12. Acceleration $\ddot{x}_n$ and velocity $\dot{x}_n$ at the maximum conveyer speed.

V. Conclusions

In this paper, a digital state-variable filter has been proposed for the generation of smooth profiles for a motion control system. The filter has been designed taking into account constraints deriving from an actual control problem.

Experimental results obtained from an actual commercial implementation of the controller have been reported. Such results show the positive effects that the proposed filter has on the controlled system: small tracking errors and reduced maximum torque values. The design of a three-order filter is under study, with the aim of imposing bounds also on the jerk signal.

Acknowledgment

The authors wish to acknowledge Eng. Zini and ARTECO s.p.a. for their fundamental support during the acquisition of the experimental results.

References

[1] C.-S. Lin, P.-R. Chang, and J. Y. S. Luh, "Formulation and optimization of cubic polynomial joint trajectories for industrial robots," *IEEE Trans. Automat. Contr.*, vol. AC-28, pp. 1066–1074, Dec. 1983.

[2] A. De Luca, L. Lanari, and G. Oriolo, "A sensitivity approach to optimal spline robot trajectories," *Automatica*, vol. 27, no. 3, pp. 535–539, 1991.

[3] C. Guarino Lo Bianco and A. Piazzi, "A semi-infinite optimization approach to optimal spline trajectory planning of mechanical manipulators," in *Semi-Infinite Programming: Recent Advances*, M. A. Goberna and M. A. López, Eds. Dordrecht, The Netherlands: Kluwer, 2001, vol. 57, Nonconvex Optimization and its Applications, ch. 13, pp. 271–297.

[4] L. R. Hunt, G. Meyer, and R. Su, "Noncausal inverses for linear systems," *IEEE Trans. Automat. Contr.*, vol. 41, pp. 608–611, Apr. 1996.

[5] G. Marro and A. Piazzi, "A geometric approach to multivariable perfect tracking," in *Proc. 13th IFAC World Congr.*, vol. C, San Francisco, CA, July 1996, pp. 241–246.

[6] A. Piazzi and A. Visioli, "Optimal noncausal set-point regulation of scalar systems," *Automatica*, vol. 37, no. 1, pp. 121–127, Jan. 2001.

[7] C. Guarino Lo Bianco, A. Tonielli, and R. Zanasi, "Nonlinear trajectory generator," in *Proc. IEEE IECON'96*, Taipei, Taiwan, R.O.C., Aug. 1996, pp. 195–201.

[8] R. Zanasi, A. Tonielli, and C. Guarino Lo Bianco, "Nonlinear filter for smooth trajectory generation," in *Proc. 4th Nonlinear Control Systems Design Symp. (NOLCOS'98)*, vol. 1, Enschede, the Netherlands, July 1998, pp. 245–250.

[9] R. Zanasi, C. Guarino Lo Bianco, and A. Tonielli, "Nonlinear filters for the generation of smooth trajectories," *Automatica*, vol. 36, no. 3, pp. 439–448, Mar. 2000.

Corrado Guarino Lo Bianco graduated with honors in electronic engineering and received the Ph.D. degree in control system engineering from the University of Bologna, Bologna, Italy, in 1989 and 1994, respectively.

Currently, he is with the Dipartimento di Ingegneria dell'Informazione, University of Parma, Parma, Italy, as a Research Associate on System Engineering. He is involved in research on variable-reluctance motors, smooth profile generation for motion control, robust control design via semi-infinite optimization, automotive applications, robotics, genetic algorithms, and interval analysis.

Roberto Zanasi (A'02) was born in Bomporto, Italy, in 1959. He graduated with honors in electrical engineering and received the Ph.D. degree in system engineering from the University of Bologna, Bologna, Italy, in 1986 and 1992, respectively.

From 1994 to 1998, he was a Researcher in Automatic Control in the Department of Electronics, Computer and System Science, University of Bologna. Since 1998, he has been an Associate Professor of Automatic Control in the Dipartimento di Ingegneria dell'Informazione, University of Modena and Reggio Emilia, Modena, Italy. He was a Visiting Scientist at the IRIMS of Moscow in 1991, at Massachusetts Institute of Technology in 1992, and at the Universite Catholique de Louvain in 1995. His research interests include linear and nonlinear control theory, mathematical modeling, simulation, variable-structure control, automotive applications, and robotics.